

Reinforcement learning to learn quantum states for Heisenberg scaling accuracy

Jeongwoo Jae,^{1,*} Jeonghoon Hong,¹ Jinho Choo,¹ and Yeong-Dae Kwon^{1,†}

¹*R&D center, Samsung SDS, Seoul, 05510, Republic of Korea*

Learning quantum states is a crucial task for realizing the potential of quantum information technology. Recently, neural approaches have emerged as promising methods for learning quantum states. We propose a meta-learning model that employs reinforcement learning (RL) to optimize the process of learning quantum states. For learning quantum states, our scheme trains a Hardware efficient ansatz with a blackbox optimization algorithm, called evolution strategy (ES). To enhance the efficiency of ES, a RL agent dynamically adjusts the hyperparameters of ES. To facilitate the RL training, we introduce an action repetition strategy inspired by curriculum learning. The RL agent significantly improves the sample efficiency of learning random quantum states, and achieves infidelity scaling close to the Heisenberg limit. We showcase that the RL agent trained using 3-qubit states can be generalized to learning up to 5-qubit states. These results highlight the utility of RL-driven meta-learning to enhance the efficiency and generalizability of learning quantum states. Our approach can be applicable to improve quantum control, quantum optimization, and quantum machine learning.

I. INTRODUCTION

Learning quantum states has emerged as a significant problem in the field of quantum computing and machine learning [1, 2]. As a tool for analyzing and benchmarking quantum systems, learning quantum states is essential for realizing quantum information technology [3]. The purpose of learning quantum states is to estimate quantum states with high fidelity based on samples obtained by measuring copies of states. Quantum state tomography (QST) is the standard method for learning quantum states [4, 5], but this method becomes impractical for large systems as the number of measurements required scales exponentially with the size of system. This limitation fuels research directions to devise various strategies for QST using matrix product state [6, 7], permutation invariance of state [8], shadow tomography [9], and Bayesian estimation [10].

With the advent of deep learning, there has been a growing body of work using a neural network-based model for learning quantum states [11–19]. Generative models provide sample-efficient methods for learning many-body quantum states based on restricted Boltzmann machine [20], variational autoencoder [21], and recurrent neural network [22]. These models are trained with unsupervised learning. Using supervised learning, a model of feed-forward neural network enhances QST by removing errors [23]. The power of these approaches stems from the *expressivity* of neural network, the ability to represent intricate features of quantum states in terms of a small number of parameters [24]. In the framework of quantum machine learning, a model based on a quantum neural network has also been employed for learning quantum systems [25–29]. The quantum model can be implemented with parameterized quantum gates [30, 31],

making it well suited for learning states of quantum computers. Moreover, it is known that a quantum neural network can have higher expressive power than classical neural networks of comparable size [32, 33].

Meanwhile, the *generalizability*, the ability to generalize to unexperienced tasks, is one of the hallmarks of machine learning model. However, some of the models for learning quantum states are difficult to generalize as each model is tailored to learning a specific quantum state. Learning models with the generalizability can be found in attempts to improve a quantum optimization algorithm using a deep learning technique [34–37]. These works employ a hybrid approach that leverages a classical model to learn a quantum model. Specifically, Verdon et al. propose a model based on a recurrent neural network to initialize the parameters of quantum approximate optimization algorithm (QAOA) circuit [35]. Similar work by Wilson et al. uses a recurrent neural network model to learn the gradient of objective function of QAOA [36]. Khairy et al. show that a feed-forward neural network model can be used to learn the hyperparameters of QAOA with reinforcement learning [37]. They show that the hybrid models can be generalized to solving problems of higher dimension than the dimension of problems for training. The deep learning technique in the previous works can be categorized as meta-learning, also called *learning to learn*, which is employed to enable a model to adapt to unexperienced tasks [38, 39]. Meta-learning methods for learning quantum states have also been proposed, where a classical model is used to learn another classical model [40] or Bayesian estimation algorithm [41]. For the task of learning quantum states, the validity and generalizability of meta-learning models in the hybrid setting remains an area of exploration.

In this work, we propose a meta-learning approach which leverages reinforcement learning (RL) to learn quantum states. The meta-learning model is based on the quantum and classical neural networks. We consider a Hardware efficient ansatz as the quantum neural network model [42]. The quantum model learns a quantum

* jeongwoo.jae@samsung.com

† y.d.kwon@samsung.com

state with a blackbox optimization algorithm, called evolution strategy (ES) [43]. To enhance the process of learning quantum states, a RL agent consisting of classical neural networks dynamically adjusts the hyperparameters of ES. We use single-shot measurements to train the quantum and classical models. It has been shown that using single-shot measurement can exhibit high shot efficiency in learning quantum states [25, 26]. To facilitate the RL, we introduce *action repetition strategy* inspired by curriculum learning, a technique for training a learning model by gradually increasing difficulty of problems [44]. The trained RL agent significantly improves the shot efficiency of learning quantum states, and enables the infidelity \bar{f} to approach the scaling of Heisenberg limit for the total number of measurement shots \mathcal{C} [45], i.e., $\bar{f} \sim \mathcal{O}(\mathcal{C}^{-1})$. We generalize the RL agent to learning quantum states of higher dimension than the dimension of quantum states used for training.

The remainder of this paper is organized as follows. We explain the scheme of meta-learning in Section II. In section III, we present results of meta-learning for random pure states, and introduce the action repetition strategy. We also investigate the generalizability of our model. We give discussion and conclusion in Section IV.

II. META-LEARNING: RL TO LEARN

The schematic of meta-learning model is illustrated in Fig. 1 (a). The environment contains an evolution strategy and a quantum system. As shown in Fig. 1 (b), the quantum system consists of a quantum state $|\psi\rangle$, a Hardware efficient ansatz (HEA) $\hat{U}(\vec{\theta})$, and a measurement. The evolution strategy trains the HEA to learn an input quantum state based on the measurement. The RL agent learns the hyperparameters of evolution strategy using two classical models in Fig. 1 (c), called *actor* and *critic*. We describe our RL scheme with a Markov decision process.

Markov decision process (MDP) is a framework to describe a sequential interaction that takes place between an environment and an agent [46]. The agent takes an action a based on observation o about the environment. As a result of an action, the state of environment is changed, and the agent receives a reward r from the environment. A purpose of agent is to learn the policy of action π to maximize cumulative rewards (see Appendix A for a detailed description).

In determining approach of agent for formulating and solving a MDP, *observability* of the environment is a significant factor to consider. When the elements of MDP are fully known, that is, assuming full observability of environment, an agent can derive the exact policy based on Bellman's principle of optimality [47]. However, in many scenarios, an agent cannot completely specify the state of environment and its dynamics due to limited (or partial) observability. Partially observable MDP (POMDP) is a generalized framework accommodating such limited ob-

servability [48]. To solve a POMDP, an agent can take a heuristic method through an iterative process. A deep RL is known as a method for learning the heuristic policies in the absence of full observability [49].

The problem we consider is the case that the RL agent does not have the full observability of environment. A quantum state transformed by the HEA, $\hat{U}(\vec{\theta})|\psi\rangle$, represents the state of environment. However, the exact state of environment is unknown to the agent, and the single-shot measurement can extract only a partial information about the quantum state. Thus, we can formulate our problem with the description of POMDP [48, 50, 51] defined by a tuple $(\mathcal{S}, \mathcal{A}, \mathcal{T}, \mathcal{R}, \Omega, \mathcal{O})$. The elements of POMDP are explained in Appendix B.

The major challenge in applying RL to quantum systems is the partial observability by quantum measurements [50]. To apply RL for control of quantum systems, there are attempts to utilize additional information about quantum states such as fidelity [52–57], but computing this quantity is typically expensive, comparable to learning quantum states by the standard QST methods. In contrast, the RL method proposed by Sivak et al. learns the control policy based on observable quantities [51]. In the same spirit, we train our RL agent using the observation o obtained by the measurement. In the following subsections, we describe in detail the configuration of environment, agent, and RL algorithm.

A. Environment

Learning a quantum state.—Consider an unknown N -qubit state $|\psi\rangle$ as the input of HEA $\hat{U}(\vec{\theta})$. We measure the quantum state transformed by the HEA, $\hat{U}(\vec{\theta})|\psi\rangle$, with a measurement $M = \{\hat{M}_s, \hat{M}_f\}$ prepared in known bases, where

$$\hat{M}_s = |s\rangle\langle s|, \quad \hat{M}_f = I - \hat{M}_s. \quad (1)$$

The outcome s stands for *success* and f does *fail*. We perform the measurement until a fail outcome appears, and count the number of success outcomes before the fail outcome. If a fail outcome appears, we change the parameters of quantum circuit based on the number of success outcomes. Otherwise, we retain the parameters. This measurement scheme is the same as that of single-shot measurement learning (SSML) [25, 26]. While SSML uses a random search algorithm to update the parameters, we use the evolution strategy which will be explained later.

We refer to the number of consecutive success outcomes as *success count*. The success count is determined by the probability of success outcome $p_s = \langle \psi | \hat{U}^\dagger(\vec{\theta}) \hat{M}_s \hat{U}(\vec{\theta}) | \psi \rangle$. Thus, the chance to obtain \mathcal{C} success count is governed by a geometric distribution

$$p(\mathcal{C}) = p_s^{\mathcal{C}}(1 - p_s). \quad (2)$$

The average value of success count is then given by $\langle \mathcal{C} \rangle = \sum_{\mathcal{C}=0}^{\infty} \mathcal{C} p(\mathcal{C}) = p_s / (1 - p_s)$. If $p_s \rightarrow 1$, $\langle \mathcal{C} \rangle \rightarrow \infty$, and, if

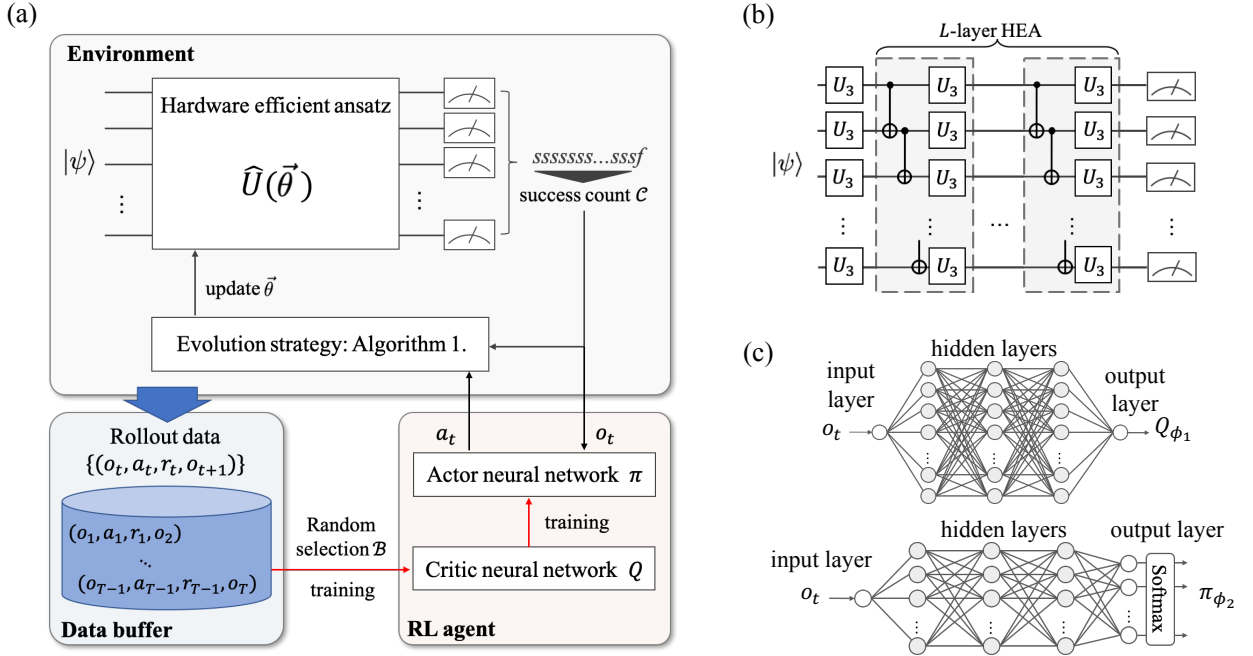


FIG. 1. Schematic of reinforcement learning to learn quantum states. (a) In the environment, the evolution strategy trains a Hardware efficient ansatz (HEA) in (b) to learn an input state $|\psi\rangle$. The observation o_t is the success count \mathcal{C} , and the HEA is trained to increase the success count. The RL agent learns the action a_t , the hyperparameters of evolution strategy, to enhance the learning quantum state. To enable the learning quantum states to be finished quickly, we give a penalty $r_t = -1$ for each time step t , and no penalty $r_t = 0$ for the time step when the learning quantum states is finished. The rollout datasets are generated by a policy-guided tree search, and stored in the data buffer. We use the Actor-Critic algorithm to train the RL agent with a subdataset \mathcal{B} randomly drawn from the buffer. (b) HEA circuit. U_3 is a generic single-qubit gate $\exp(i\vec{\theta} \cdot \vec{\sigma}/2)$, where $\vec{\theta} = (\theta_x, \theta_y, \theta_z)$ and $\vec{\sigma}$ is a vector of Pauli operators $(\hat{\sigma}_x, \hat{\sigma}_y, \hat{\sigma}_z)$. For 1-qubit states, we use a single U_3 gate. For N -qubit states, we use a HEA of L layers which has $3N(L+1)$ parameters. (c) Feed-forward neural networks for the RL agent. The input of each network is the observation o_t . Q_{ϕ_1} is the observation-value function and π_{ϕ_2} is the policy of action.

$p_s = 0$, $\langle \mathcal{C} \rangle = 0$. The success count is the observation o , and the geometric distribution determines the transition probability of observation.

We train the HEA until the success count achieves a high value so that the HEA transforms the input quantum state close to the basis of success outcome. We set a target success count $\mathcal{C}_{\text{target}}$, and have the training process stop if a success count reaches or exceeds the target value, i.e., $\mathcal{C} \geq \mathcal{C}_{\text{target}}$. The value of target success is related to the accuracy of reconstructed quantum state.

Quantum state reconstruction.—After the training, we can reconstruct the input quantum state through the trained HEA as

$$|\psi_{\text{est}}\rangle = \hat{U}^\dagger(\vec{\theta}_{\text{train}})|s\rangle. \quad (3)$$

To assess the accuracy of the reconstructed state $|\psi_{\text{est}}\rangle$, we choose the *infidelity* as a figure of merit [45] defined by

$$\bar{f} := 1 - |\langle \psi | \psi_{\text{est}} \rangle|^2 \quad (4)$$

The infidelity depends on the target success count $\mathcal{C}_{\text{target}}$ we initially set; The larger the target success count, the better the accuracy of the estimation.

Optimizer.—To train the HEA, we employ an evolution strategy (ES) [58]. An ES consists of following steps: (i) assuming a probability distribution for sampling, (ii) sampling parameters around a current parameter, (iii) evaluating the parameter samples, and (iv) updating the current parameter based on the evaluations. In our problem, the ES uses a multivariate Gaussian distribution to sample parameters [43], and the evaluation corresponds to measuring the success count.

The purpose of ES is to find the parameters of HEA $\vec{\theta}$ to achieve the halting condition $\mathcal{C}(\vec{\theta}) \geq \mathcal{C}_{\text{target}}$. For this purpose, we consider the expectation of success count as an objective function of ES

$$J(\vec{\theta}) := \frac{1}{\mathcal{C}_{\text{target}}} \mathbf{E}_{\vec{\theta} \sim p(\vec{\theta})} [\mathcal{C}(\vec{\theta})], \quad (5)$$

where the target success count $\mathcal{C}_{\text{target}}$ is introduced in the denominator to normalize the objective function. $p(\vec{\theta})$ is the multivariate Gaussian distribution $\mathcal{N}(\vec{\theta}, \sigma^2 I)$ of mean $\vec{\theta}$ and covariance matrix $\sigma^2 I$, where $\sigma \in (0, \infty)$ is a hyperparameter to determine the *range of sampling* over the space of parameters, and I is the identity matrix.

To increase the expected success count, the parameters

Algorithm 1 Evolution strategy with RL agent

```

1: Set an input quantum state  $|\psi_1\rangle$ , the HEA  $\hat{U}(\vec{\theta}_0)$ , the
   target success count  $\mathcal{C}_{\text{target}}$ , the number of samples  $k$ , and
   the RL agent  $\pi$ 
2: for  $t = 1, 2, \dots, t_{\text{max}}$  do
3:   Measure  $\mathcal{C}(\vec{\theta}_t)$  and  $o_t \leftarrow \mathcal{C}(\vec{\theta}_t)$ 
4:   Draw  $\sigma_t$  and  $\eta_t$  from the agent, i.e.,  $(\sigma_t, \eta_t) \sim \pi(a_t|o_t)$ 
5:   Sample  $\vec{\epsilon}_1, \dots, \vec{\epsilon}_k \sim \mathcal{N}(0, I)$ 
6:   Measure  $\mathcal{C}(\vec{\theta}_t + \sigma_t \vec{\epsilon}_i)$  for  $i = 1, \dots, k$ 
7:   if any  $\mathcal{C} \geq \mathcal{C}_{\text{target}}$  then
8:     break
9:   end if
10:   $\vec{\theta}_{t+1} \leftarrow \vec{\theta}_t + \eta_t \nabla_{\vec{\theta}} \tilde{J}(\vec{\theta}_t)$  ▷ Eq. (7)
11:   $|\psi_{t+1}\rangle \leftarrow \hat{U}(\vec{\theta}_{t+1}) |\psi_1\rangle$ 
12: end for
13:  $\mathcal{C}_{\text{total}} \leftarrow$  the sum of success counts
14:  $t_H \leftarrow t$ 
15:  $\vec{\theta}_{\text{train}} \leftarrow \vec{\theta}$  s.t.  $\mathcal{C}(\vec{\theta}) \geq \mathcal{C}_{\text{target}}$ 

```

are updated by following rule

$$\vec{\theta} \leftarrow \vec{\theta} + \eta \nabla_{\vec{\theta}} \tilde{J}(\vec{\theta}), \quad (6)$$

where $\eta \in [0, \infty)$ is the *learning rate*, and $\nabla_{\vec{\theta}} \tilde{J}(\vec{\theta})$ is an estimator of gradient. Applying the reparameterization trick [43], the ES estimates the gradient by drawing $\{\vec{\epsilon}_i\}_{i=1}^k$ from a distribution $\mathcal{N}(\vec{0}, I)$, and evaluating k parameter samples $\{\vec{\theta} + \sigma \vec{\epsilon}_i\}_{i=1}^k$. The estimator of gradient is given by

$$\nabla_{\vec{\theta}} \tilde{J}(\vec{\theta}) = \frac{1}{\mathcal{C}_{\text{target}} \sigma k} \sum_{i=1}^k \mathcal{C}(\vec{\theta} + \sigma \vec{\epsilon}_i) \vec{\epsilon}_i. \quad (7)$$

The hyperparameter of sampling range, also called step size, is a significant factor to determine the performance of ES. The sampling range decides the range of search: A larger sampling range induces more exploration on the parameter space. A smaller sampling range focuses on exploitation, searching in a narrower region to enhance solution. In advanced variants of ES such as covariance matrix adaptation ES [59], the sampling range and learning rate are dynamically adjusted, and their combination determines the covariance matrix (or the inverse of Hessian matrix) which reflects the local geometry of objective function. In our scheme, the sampling range σ and learning rate η are dynamically changed according to the policy π .

The pseudocode of ES is shown in Algorithm 1. Unlike the two hyperparameters σ and η , we fix the number of samples k to a single value to keep the statistical uncertainty of the gradient estimator at a certain degree during the execution of ES. $\mathcal{C}_{\text{total}}$ is the total success count used, and the halting time, t_H , is the time steps taken until the training is finished. Note that the time here means that how many loops the ES takes until the success count reaches the halting condition $\mathcal{C} \geq \mathcal{C}_{\text{target}}$. In a real experiment, the total success count is a quantity which is proportional to physical runtime for the training.

An optimizer typically used to train a quantum neural network is a gradient method [60, 61], but it can suffer the gradient vanishing problem, called barren plateau [62, 63], making the training intractable. While the gradient vanishing effect cannot be fully alleviated [64], recent studies have shown that an ES can be useful for training some cases of quantum neural networks [65, 66]. The gradient methods typically require more evaluation points than parameters to obtain directional derivatives [60]. In contrast, we will show that the ES can train the HEA with the fewer evaluations than the parameters of HEA.

B. RL agent

The RL agent consists of an actor and a critic, both implemented by feed-forward neural networks [see Fig. 1 (c)]. The both networks use three hidden layers. For each hidden layer, the critic has hundred nodes, and the actor has fifty nodes. We use ReLu for activation functions. The actor is to learn a policy of action. We construct the action space \mathcal{A} by selecting m values from each of the hyperparameter spaces $\mathcal{A}_\sigma = [0, \infty)$ and $\mathcal{A}_\eta = [0, \infty)$. So the number of actions the agent can choose from is $m^2 = |\mathcal{A}|$. The output of actor is the policy $\pi_{\phi_2} = p(\sigma, \eta|o, \phi_2)$, the probability distribution defined over the action space \mathcal{A} . The critic outputs an estimate of observation-value function $Q_{\phi_1}(o)$.

We train the agent to recommend the hyperparameters σ and η that enables the learning quantum states to be finished quickly. This is accomplished by giving a penalty of -1 for each time step, and no penalty for the time step when the learning quantum states is finished. In other words, the reward is given by

$$r_t = \begin{cases} 0 & \text{if } t = t_H \\ -1 & \text{otherwise.} \end{cases} \quad (8)$$

The empirical cumulative reward is then given by

$$\mathcal{R}_t = \sum_t^{t_H} r_t = t - t_H. \quad (9)$$

For the training, we use the Actor-Critic algorithm, and collect training datasets using a tree search guided by the policy. See Appendix C for detailed description.

III. RESULTS

A. Training RL agent

We apply our meta-learning scheme to learning random pure states. The random states are prepared by acting unitary operators \hat{V} s drawn from Haar measure to a computational basis state $|0\rangle$ [67]. To measure these states, we perform a measurement in the computational basis, and consider that the basis $|0\rangle\langle 0|^{\otimes N}$ is the basis of

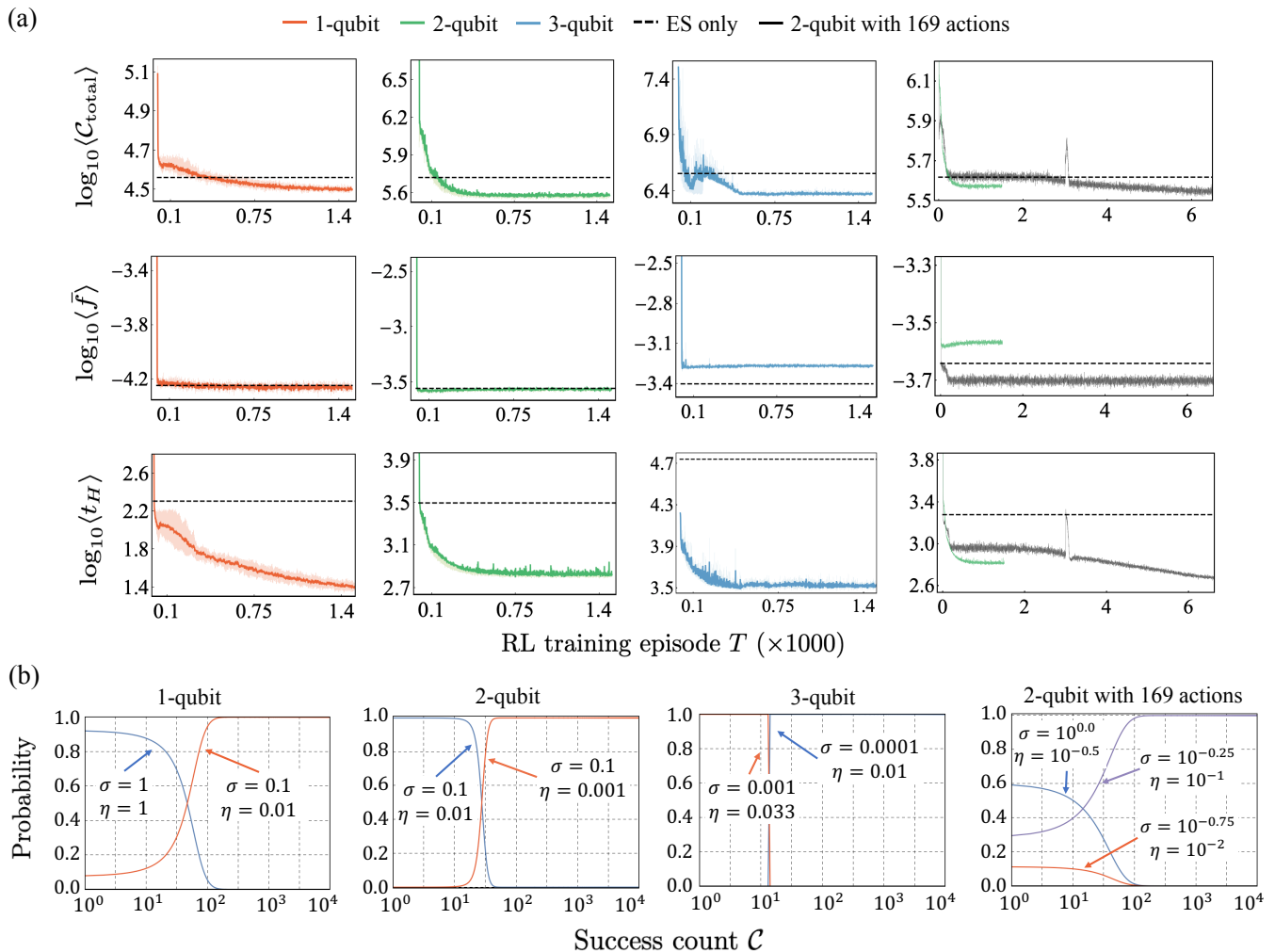


FIG. 2. Results of training RL agent for the target success count $C_{\text{target}} = 10^4$. For each RL training episode T , we perform learning a thousand random states. $\langle C_{\text{total}} \rangle$ is the average of total success count. $\langle \bar{f} \rangle$ is the average infidelity of learned states. $\langle t_H \rangle$ is the average halting time steps of evolution strategy. (a) The red, green, and blue solid lines are the training curves for learning 1-, 2-, and 3-qubit states with the 16 actions. The black solid line is obtained by using the extended action space for learning 2-qubit states. The dashed lines are baseline values. (b) The policy of trained RL agent.

success outcome $|s\rangle\langle s|$. For each RL episode T , we prepare a new thousand problem instances, and execute the learning quantum states to collect datasets for training the RL agent. We obtain following results through simulations implemented with PyTorch [68] on four NVIDIA Tesla A100 graphic processing units (GPUs). Code is available at Ref. [69].

We present the setting of HEA, the number of samples, and the space of action in Table I. While the number of parameters of unitary operator required to prepare an N -qubit state is 4^N , we show that the HEA can learn the random quantum states with fewer parameters: For the learning 2- and 3-qubit states, we use the HEAs which have 12 and 54 parameters, respectively. We will also show that HEA of 10 layers can learn random 4- and 5-qubit states. Moreover, to estimate the gradient of HEAs, we use fewer samples than the parameters of HEA cir-

cuits. For 2- and 3-qubit states, the number of samples is set to 10 and 30, respectively.

The results of training RL agent are illustrated in Fig. 2 (a). For these results, we set the target success count to $C_{\text{target}} = 10^4$, and randomly initialize the parameters of HEAs. We compare these results to the performance obtained without the RL, i.e., using only a single action for the entire process of learning quantum states. We regard results obtained from an action which gives the lowest total success count as baseline values, and train the RL agent until it outperforms the baseline values. The baselines are selected based on data in Appendix. D.

At the end of RL training ($T \approx 1500$), the average of total success counts required to learn the 1-, 2-, and 3-qubit states are 3.123×10^4 , 3.767×10^5 , and 2.363×10^6 , which are about 14%, 28%, and 34% lower than the baseline values, respectively. Using the RL, we obtain the

TABLE I. The settings used to train the RL agent. The space of action is given by $\mathcal{A} = \mathcal{A}_\sigma^4 \times \mathcal{A}_\eta^4$. The action repetition time t_{rep} is determined by the parameters $(t_l, t_u, T_{\text{th}})$. For 4- and 5-qubit, we perform the learning random pure states with the RL agent trained using the 3-qubit states.

No. qubits N	Quantum neural network	No. samples k	The space of sampling range \mathcal{A}_σ^4	The space of learning rate \mathcal{A}_η^4	Action repetition strategy $(t_l, t_u, T_{\text{th}})$
1	U_3	5	{1.0, 0.1, 0.01, 0.001}	{1.0, 0.1, 0.01, 0.001}	(1, 50, 100)
2	HEA, $L = 1$	10	{1.0, 0.1, 0.01, 0.001}	{1.0, 0.1, 0.01, 0.001}	(80, 800, 100)
3	HEA, $L = 5$	30	{0.1, 0.01, 0.001, 0.0001}	{1.0, 0.33, 0.01, 0.033}	(300 ^a , 2000, 500)
4	HEA, $L = 10$	100	{0.1, 0.01, 0.001, 0.0001}	{1.0, 0.33, 0.01, 0.033}	$t_{\text{rep}} = 300$
5	HEA, $L = 10$	100	{0.1, 0.01, 0.001, 0.0001}	{1.0, 0.33, 0.01, 0.033}	$t_{\text{rep}} = 300$

^a We obtain similiar results for $t_l = 200$.

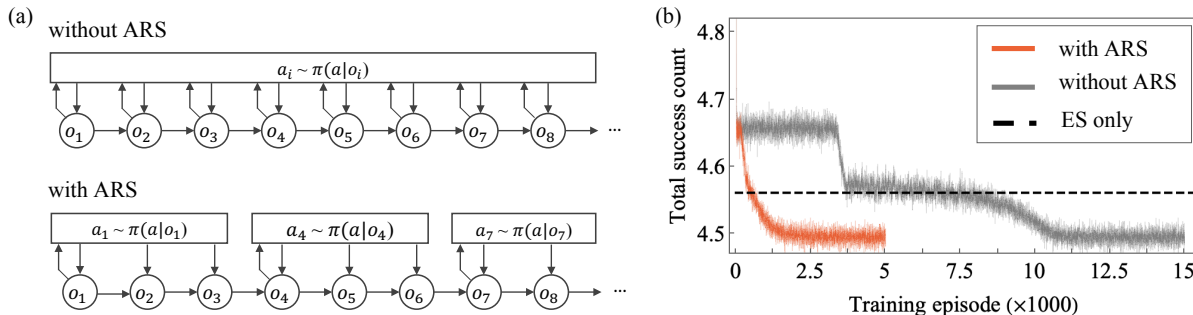


FIG. 3. (a) The scheme of action repetition strategy (ARS). If the ARS is not applied, the agent π draws a new action a_i based on the observation o_t at each time step. With the ARS, the agent repeats an action chosen during t_{rep} time steps. The example shows the case of $t_{\text{rep}} = 3$. (b) Learning random 1-qubit states with and without ARS. The red solid line is obtained by using the ARS with setting $(t_u, t_l, T_{\text{th}}) = (50, 1, 100)$. The gray solid line is obtained without the ARS. The dashed line is the baseline value (ES only).

(in) fidelity similar to the baselines, except for the case of 3-qubit. The average fidelity is given by 0.99994, 0.99972, and 0.99946 for 1-, 2-, and 3-qubit states, respectively. In the early episodes of RL, the average halting time t_H of learning 1-, 2-, and 3-qubit states is about 10^3 , 10^4 , and 1.5×10^4 , and these are reduced to 19, 660, and 3409 at the end of episode, respectively. For these results, we use the 16 actions defined in Table I.

For the 2-qubit states, we also consider an extended action space defined by $\mathcal{A} := \mathcal{A}_\sigma^{13} \times \mathcal{A}_\eta^{13}$, where

$$\mathcal{A}_\sigma^{13} = \left\{ \sigma_i \mid \sigma_i = 10^{-0.25(i-1)} \text{ for } i = 1, \dots, 13 \right\} \quad (10)$$

$$\mathcal{A}_\eta^{13} = \left\{ \eta_i \mid \eta_i = 10^{-0.25(i-1)} \text{ for } i = 1, \dots, 13 \right\}.$$

The number of actions in the extended space is 169. Except for the number of actions, we use the same settings for the 2-qubit case listed in Table I. The result is shown in the rightmost column of Fig. 2 (a). By extending the action space, we can attain the lower values of average total success count and infidelity than the case of using the 16 actions. The average total success count is 3.593×10^5 and the average fidelity is 0.9998. To achieve these results, on average, 433 time steps are required. While the overall performance of learning 2-qubit states is improved

by extending the action space, the agent requires more episodes to be trained.

Fig. 2 (b) shows the policy of trained actor. These policies imply that the trained RL agent takes a strategy; if the success count is small, the agent recommends the large values for σ and η to enable the ES to search in a wide range of parameter space; if the success count is large, the agent reduces the values of recommended hyperparameter to make the learning quantum states to converge.

B. Action repetition strategy

To obtain these results, we use a method, called *action repetition strategy* (ARS), that repeats an action given by the RL agent for a certain period of time steps t_{rep} . The schematic of ARS is illustrated in Fig. 3 (a). For each RL episode T , t_{rep} is given by

$$t_{\text{rep}} = \max \left(\left\lceil t_u - \frac{T}{T_{\text{th}}} (t_u - t_l) \right\rceil, t_l \right), \quad (11)$$

where t_u and t_l are the upper and lower value of t_{rep} , respectively, and $t_u > t_l$. When $T = 0$, the action repetition time is t_u , and it decreases until the RL episode T reaches T_{th} . After T_{th} , t_{rep} saturates to t_l .

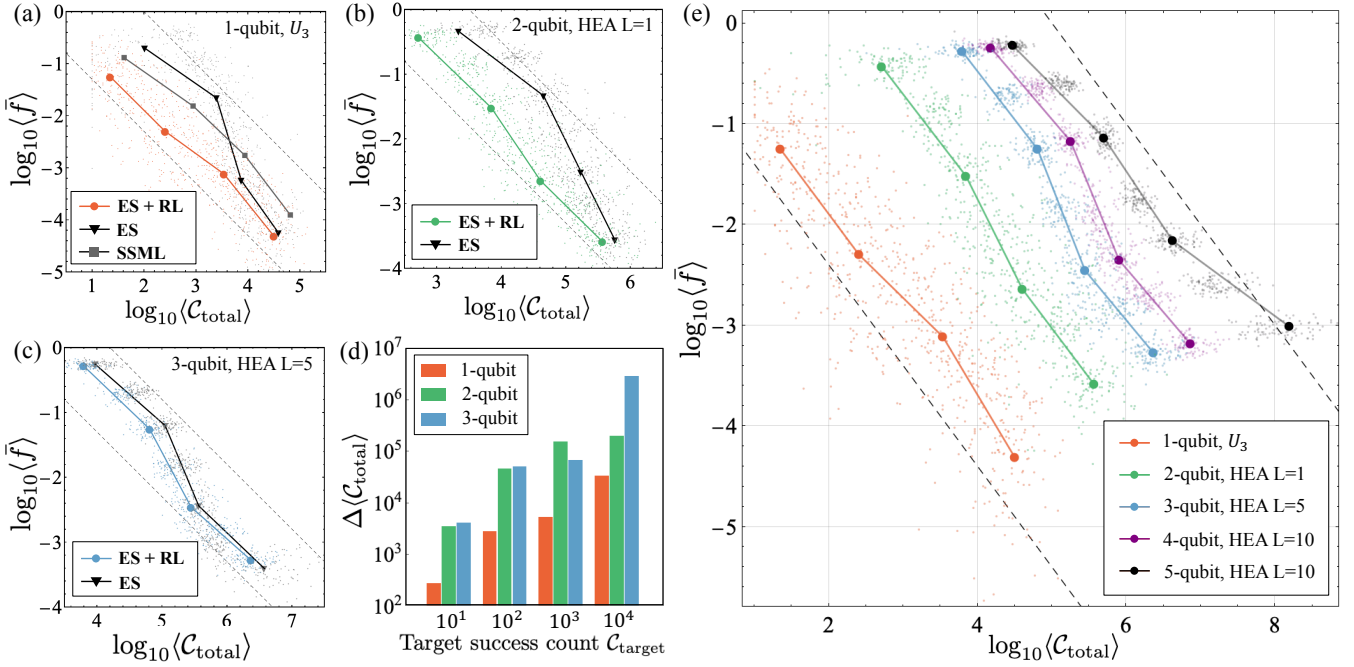


FIG. 4. Learning random pure states with trained RL agent. We consider the target success counts from 10^1 to 10^4 . The dots in (a)–(c) and (e) represent the average total success count $\langle C_{\text{total}} \rangle$ and the average infidelity $\langle \bar{f} \rangle$ for the learning 1-qubit (red), 2-qubit (green), and 3-qubit (blue) states. We denote the results obtained using the trained RL agent, referred to as **ES+RL**. The black triangles are the average values obtained without the RL agent, which are denoted by **ES**. For the results of **ES**, we use an action a_{base} which gives the baseline values. **SSML** denotes the results obtained by the single-shot measurement learning. (d) $\Delta \langle C_{\text{total}} \rangle = \langle C_{\text{total}} \rangle_{\text{ES}} - \langle C_{\text{total}} \rangle_{\text{ES+RL}}$ is the amount of average total success counts reduced by using the trained RL agent. (e) The purple and black dots are results of generalizing the RL agent trained using 3-qubit states to learning random 4- and 5-qubit states, respectively. The dashed lines represent the scaling of statistical limit, $\bar{f} \sim \mathcal{O}(C_{\text{total}}^{-1})$.

The ARS is a method inspired by *curriculum learning*, a technique that trains a machine learning model by gradually increasing the difficulty of problems [44]. Note that the curriculum learning belongs to the category of transfer learning, which reuses a model or knowledge obtained from a task to learn a related task [70–72]. One of factors that determines the difficulty of RL problem is the depth of decision process. In general, the deeper the decision process, the more difficult the problem is considered to be. The depth of decision process of our problem t_H in the early episodes is about 10^3 , 10^4 , and 1.5×10^4 for the learning 1-, 2-, and 3-qubit states, respectively. With the ARS, we can reduce the depth of decision process to $\lfloor t_H/t_{\text{rep}} \rfloor$, which is shallower than the original depth. Specifically, according to the settings in Table I, the decision process can be reduced to tens of steps in the beginning of the RL training. This leads to the significant decrease of difficulty of problem. As the RL training proceeds, the difficulty of problem increases again with the decrease of t_{rep} . Thus, by controlling the action repetition time, the ARS enables the RL agent to experience problems of various difficulty levels during the training process.

For the random 1-qubit states, we compare the performance obtained with and without the ARS in Fig 3 (b). With the ARS, the RL agents can converge faster

than the case without the ARS. For the random 2- and 3-qubit states, the training RL agent without the ARS requires computational resources far exceed our capacity. In some intervals of RL episodes, the difficulty of our problem does not gradually increase since the halting time step t_H also decreases together with the action repetition time. More sophisticated curriculum for the repetition time may improve the performance of meta-learning, but it is beyond the scope of this work and remains an open question.

C. The scaling of infidelity

Using the RL agents trained with the target success count $C_{\text{target}} = 10^4$, we perform the learning a hundred random pure states by varying the target success counts from 10^1 to 10^4 . The results are shown in Fig. 4 (a)–(c). We compare these results to the baseline values obtained by an action a_{base} (see Appendix D). Fig. 4 (d) shows the amount of total success counts saved by the RL agent according to the increase of the number of qubits N and target success count C_{target} . The amount of total success counts saved is represented by $\Delta \langle C_{\text{total}} \rangle := \langle C_{\text{total}} \rangle_{\text{ES}} - \langle C_{\text{total}} \rangle_{\text{ES+RL}}$, where $\langle C_{\text{total}} \rangle_{\text{ES}}$ is obtained using a_{base} without the RL agent, and $\langle C_{\text{total}} \rangle_{\text{ES+RL}}$ is

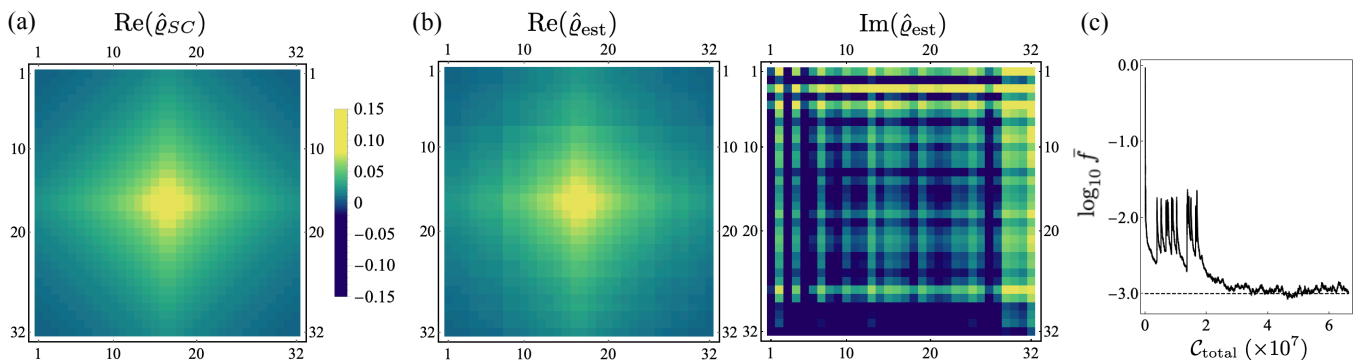


FIG. 5. Learning an entangled 5-qubit pure state $\hat{\rho}_{SC}$ with the RL agent trained using the random 3-qubit states. (a) $\text{Re}(\hat{\rho}_{SC})$ represents the real parts of density matrix of 5-qubit state. The imaginary parts of density matrix are zero. (b) The reconstructed state $\hat{\rho}_{est}$ of the 5-qubit state. $\text{Re}(\hat{\rho}_{est})$ and $\text{Im}(\hat{\rho}_{est})$ represent real and imaginary parts of density matrix $\hat{\rho}_{est}$, respectively. The reconstructed state achieves the fidelity $f \approx 0.9989$. (c) The changes of infidelity during the entire learning process.

the average total success count obtained with the trained RL agent. In the target success count 10^4 , $\Delta\langle C_{total} \rangle$ is given by 3.274×10^4 , 1.995×10^5 , and 2.818×10^6 for 1-, 2-, and 3-qubit states, respectively. This leads to enhancement in the scaling of average infidelity \bar{f} versus the total success counts C_{total} . The scaling nearly achieves the Heisenberg limit [45], $\bar{f} \sim \mathcal{O}(C_{total}^{-1})$, which the standard QST method cannot attain without additional information about quantum states [73].

We curve fit the results of Fig. 4 (a)–(c) with $\bar{f} = \alpha C_{total}^{-\beta}$. The scaling factor is given by $\beta \approx 0.948$, 1.161, and 1.184 for the learning 1-, 2-, and 3-qubit states, respectively. Our method shows the similar results to previous works on learning 1-qubit states [25, 26, 74–76], where the scaling factors lie in the range $\beta \in [0.9, 1.0]$. Typically, the SSML shows the scaling of $\beta \approx 0.972$ in our simulation, which is consistent with the results in their works [25, 26]. (In the multi-qubit cases, we fail to find hyperparameter settings of SSML to achieve the optimal scaling.) Our result obtained with the RL agent achieves the similar scaling factor while using fewer total success count than the SSML as shown in Fig. 4 (a).

D. Generalization of RL agent

We apply the RL agent trained with the random 3-qubit states to learning a hundred random 4- and 5-qubit states. The results are illustrated in Fig. 4 (e). For the target success count $C_{target} = 10^4$, the average of total success count and infidelity are given by $\langle C_{total} \rangle \approx 7.261 \times 10^6$ and $\bar{f} \approx 6.561 \times 10^{-4}$ for 4-qubits, and $\langle C_{total} \rangle \approx 1.291 \times 10^8$ and $\bar{f} \approx 9.311 \times 10^{-4}$ for 5-qubits. The scaling factor of infidelity achieves $\beta = -1.189$ and $\beta = -0.829$ for 4- and 5-qubit, respectively. For the multi-qubit cases including 2- and 3-qubit results, our method gives the similar results to the self-guided quantum state tomography (SGQT) which shows the scaling factors in the range $\beta \in (0.80, 1.05)$ up to 10-qubits [76].

By using the trained RL agent, we learn a specific 5-qubit state, and reconstruct the learned state. As illustrated in Fig. 5 (a), the density matrix of 5-qubit state $\hat{\rho}_{SC}$ is given by a Shen-Castan matrix of which element is determined by a real-valued function $\exp[-(|m - 16.5| + |n - 16.5| + 1)/10]/K$ for $m, n = 1, \dots, 32$ and $K = 0.00366$. (A Shen-Castan matrix is a filter used for edge detection in image processing [77].) This quantum state is pure, i.e., $\text{Tr} \hat{\rho}_{SC}^2 = 1$, and the five qubits are entangled. For a reduced state of i -th subsystem $\hat{\rho}_i$, Von Neumann entropy $S_i := -\text{Tr} \hat{\rho}_i \log_2 \hat{\rho}_i$ has nonzero value: $S_1 = 0.640$, $S_2 = 0.547$, $S_3 = 0.230$, $S_4 = 0.080$, and $S_5 = 0.025$. In the learning of the 5-qubit state, we achieve the fidelity $f \approx 0.9989$ by using 6.62×10^7 success count. The result of state reconstruction is illustrated in Fig. 5 (b). Fig. 5 (c) shows the changes of infidelity during the learning process. The policy of RL agent induces exploration in the early time steps, and, as the ES approaches the optimal point, the agent focuses on exploitation to improve the quality of solution.

IV. DISCUSSION & CONCLUSION

The single-shot measurement scheme used in this work is proposed by the single-shot measurement learning (SSML) [25, 26]. Notably, the SSML addresses following problems of the standard approach: (i) The way to reconstruct a learned state is not known. (ii) The learned state can have negative eigenvalues [5]. (iii) The scaling of infidelity is limited to $\mathcal{O}(n^{-3/4})$ for n copies of states without additional information about quantum state [73]. Our method also does not suffer from these problems. The trained HEA immediately provides a way to reconstruct the estimated state, and the reconstructed state always satisfies the conditions of quantum state as the state reconstruction is given by the quantum circuit. Also, the average infidelity nearly achieves the scaling of statistical limit [45]. While the SSML shows that the optimal scaling in the learning up to 6-dimensional states, our

results show the optimal scaling for higher dimensional states. Implementing the SSML on a quantum computer is difficult for high-dimensional states as it uses a parameterized special unitary gate and compiling the parameterized circuit typically incurs a high computational cost. In our method, we use the Hardware efficient ansatz of which structure can be compatible with quantum computers of low connectivity, e.g., one-dimensional array of qubits allowing neighborhood interaction.

A strategy of action repetition has been used in a reinforcement learning scheme for games [78]. In this context, the motivation of action repetition is to imitate human behaviors in playing games. On the other hand, we use the action repetition strategy to control the depth of decision process with the curriculum so that the agent can experience the problems of various difficulties. Reducing the depth and breadth of the decision process is a key issue in successfully applying reinforcement learning to large-scale problems [79]. (Note that, in our problem, the discretization of action space plays a role in reducing the breadth of decision process.) The efficacy of curriculum learning has been shown in meta-learning schemes for gradient descents [39] and the quantum optimization problems [36]. In the setting of our problem, the curriculum of the previous works can be realized by gradually increasing the maximum time steps of evolution strategy from a small value to a large value. However, we do not apply this curriculum to our method as the control of maximum time step directly affects the estimation accuracy of observation-value function. We estimate the value function based on the empirical cumulative reward, and we require the learning quantum state to be completed within a maximum time step to accurately compute the cumulative reward. If the maximum time step is set to a small value, the learning process will not be completed, and this hinders the calculation of cumulative reward. The inaccurate estimation of value function can bias the agent to only solve easy problem instances, the quantum states which can be learned in a short time step.

For the task of learning quantum states, we propose the meta-learning scheme based on the hybrid model of quantum and classical neural networks. We perform the learning Haar-random quantum states by training the Hardware efficient ansatz (HEA) of low connectivity with the evolution strategy. To improve the learning quantum states, we use the reinforcement learning (RL), and the RL agent learns the policy to dynamically adjust the hyperparameters of evolution strategy. The trained RL agent enables the infidelity of reconstructed states to approach the scaling of Heisenberg limit [45]. Our meta-learning model demonstrates the generalizability by showing that the RL agent can be applicable to learning quantum states of higher dimension than the dimension of quantum states used for training. The generalization is possible since the structure of RL agent is independent of the dimension of quantum system. To obtain these results, we introduce the action repetition strategy (ARS) which can facilitate the training of RL agent. We

expect that our meta-learning scheme including the ARS can be leveraged to improve known classical and quantum algorithms for learning quantum states, quantum control [80], quantum machine learning [81], and quantum optimization [34, 82]. Furthermore, hyperparameter optimization and improving blackbox optimization algorithms through meta-learning have broad applications across disciplines [36, 83–86].

ACKNOWLEDGMENTS

Authors thank Minyoung Lee and Taehee Lee for their support. J.J. thanks Sang Min Lee and Jeongho Bang for discussions.

Appendix A: Markov decision process

For finite time steps $t = 1, 2, \dots, T$, a markov decision process (MDP) is represented by a tuple $(\mathcal{S}, \mathcal{A}, \mathcal{T}, \mathcal{R})$, where \mathcal{S} is the space of state s_t , \mathcal{A} is the space of action a_t , \mathcal{T} is the space of transition probability $p(s_{t+1}|s_t, a_t)$ from a state s_t to s_{t+1} by an action a_t , and \mathcal{R} is the space of reward r_t . In the description of MDP, a trajectory of decision process τ , e.g., $s_1, a_1, r_1, \dots, s_{T-1}, a_{T-1}, s_T, r_T$, is deemed to satisfy Markov condition, which assumes that a current state and reward only depend on a previous state and action. Specifically, the assumption implies that a probability distribution which governs the trajectory τ can be written as

$$\begin{aligned} p(\tau) &= p(s_1, a_1, r_1, s_2, a_2, r_2, \dots, s_{T-1}, a_{T-1}, s_T, r_T) \\ &= p(s_1) \prod_{t=1}^{T-1} p(s_{t+1}, r_{t+1} | s_t, a_t) p(a_t | s_t), \end{aligned} \quad (\text{A1})$$

where the probability $p(a_t | s_t)$ is called *policy*. The purpose of agent is to learn the optimal policy so as to maximize the expected cumulative reward G_t at each time step t , where

$$G_t := \mathbf{E}_{\tau \sim p(\tau)} \left[\sum_t^T r_t \right]. \quad (\text{A2})$$

Finally, the RL problem that the agent solves is an optimization to find a policy $\tilde{\pi}$ such that

$$\tilde{\pi} = \operatorname{argmax}_{\{p(a_t | s_t)\}} G_0. \quad (\text{A3})$$

Appendix B: Elements of POMDP

Our RL problem can be formulated with a POMDP defined by a tuple $(\mathcal{S}, \mathcal{A}, \mathcal{T}, \mathcal{R}, \Omega, \mathcal{O})$:

1. \mathcal{S} is the Hilbert space of N -qubit states. The state s_t is a quantum state $\hat{U}(\vec{\theta}_t) |\psi\rangle$ transformed by the HEA in Fig. 1 (b).

(a) 1-qubit					(b) 2-qubit					(c) 3-qubit					(d) 2-qubit with 169 actions											
Total success count					Total success count					Total success count					Total success count											
$\sigma \backslash \eta$	0.001	0.01	0.1	1	$\sigma \backslash \eta$	0.001	0.01	0.1	1	$\sigma \backslash \eta$	0.0001	0.001	0.01	0.1	$\log_{10} \sigma \backslash \eta$	-0.75	-1	-1.25	-1.5	-1.75	-2	-2.25	-2.5	-2.75	-3	
0.001	5.444	5.173	5.143	5.152	0.001	7.002	7.006	7.006	7.006	0.001	0.0001	0.001	0.01	0.1	0	7.076	7.084	7.090	7.099	7.105	7.106	7.111	7.108	7.102	7.091	
0.01	5.199	5.255	5.139	5.133	0.01	7.060	7.005	7.008	7.008	0.01	0.033	6.509	7.740	8.004	-0.25	7.159	7.191	7.149	7.043	7.045	7.106	7.208	7.294	7.329	7.362	
0.1	4.967	4.562	4.825	4.886	0.1	5.733	6.411	7.050	7.014	0.01	0.33	8.125	8.163	8.114	-0.5	7.191	7.262	7.224	6.906	6.415	6.134	6.034	6.081	6.280	6.444	
1	4.835	4.903	4.743	4.659	1	7.092	7.109	7.084	7.046	1	8.006	8.006	8.006	8.006	-0.75	7.085	7.194	7.354	7.230	6.631	6.113	5.776	5.686	5.779	5.950	
															-1	7.024	7.049	7.116	7.312	7.261	6.481	5.907	5.654	5.618	5.752	
															-1.25	7.010	7.014	7.026	7.056	7.145	7.288	6.458	5.830	5.625	5.706	
															-1.5	7.008	7.007	7.008	7.014	7.027	7.060	7.155	6.633	5.845	5.707	
															-1.75	7.009	7.007	7.005	7.005	7.008	7.014	7.028	7.058	7.101	6.061	
Infidelity					Infidelity					Infidelity					Infidelity											
0.001	-2.344	-3.610	-3.824	-3.779	0.001	-0.014	-0.035	-0.038	-0.034	0.001	0.0001	0.001	0.01	0.1	0	-0.946	-1.039	-1.108	-1.170	-1.194	-1.206	-1.227	-1.226	-1.226	-1.197	
0.01	-4.009	-3.348	-3.832	-3.895	0.01	-0.302	-0.032	-0.047	-0.052	0.01	0.033	-3.391	-3.319	-0.389	-0.041	-0.25	-1.281	-1.543	-1.987	-2.441	-2.615	-2.511	-2.386	-2.314	-2.301	-2.265
0.1	-4.248	-4.262	-4.231	-4.265	0.1	-3.558	-3.620	-0.269	-0.087	0.01	0.33	-3.489	-0.361	-0.035	-0.030	-0.5	-0.962	-1.403	-2.118	-3.228	-3.608	-3.601	-3.551	-3.468	-3.368	-3.298
1	-4.226	-4.216	-4.224	-4.248	1	-1.201	-1.205	-1.034	-0.542	1	8.006	8.006	8.006	8.006	-0.75	7.085	-0.779	-1.379	-2.682	-3.631	-3.622	-3.629	-3.599	-3.505	-3.431	
															-1	-0.143	-0.278	-0.510	-1.037	-2.930	-3.621	-3.639	-3.675	-3.641	-3.549	
															-1.25	-0.066	-0.096	-0.154	-0.292	-0.565	-1.995	-3.621	-3.663	-3.707	-3.685	
															-1.5	-0.051	-0.048	-0.054	-0.093	-0.153	-0.287	-0.641	-3.614	-3.656	-3.712	
															-1.75	-0.052	-0.044	-0.032	-0.034	-0.052	-0.088	-0.165	-0.297	-0.922	-3.643	
Total time steps					Total time steps					Total time steps					Total time steps											
0.001	0.6136	0.2623	0.1853	0.2004	0.001	1	1	1	1	0.001	0.0001	0.001	0.01	0.1	0	0.999	0.998	0.996	0.997	0.998	0.998	0.997	0.999	0.997	1	
0.01	0.0908	0.4200	0.2227	0.1672	0.01	0.999	1	1	1	0.01	0.033	0.055	1	1	-0.25	0.996	0.984	0.915	0.779	0.729	0.751	0.813	0.874	0.891	0.925	
0.1	0.0159	0.0018	0.0185	0.0765	0.1	0.031	0.063	1	1	0.01	0.33	0.997	0.989	1	-0.5	0.999	0.986	0.881	0.525	0.148	0.058	0.039	0.047	0.073	0.119	
1	0.0174	0.0071	0.0019	0.0017	1	1	0.999	0.998	1	1	1	1	1	1	-0.75	1	0.999	0.977	0.704	0.182	0.039	0.017	0.017	0.026	0.043	
															-1	1	1	0.999	0.990	0.614	0.069	0.016	0.013	0.019	0.032	
															-1.25	1	1	1	1	0.997	0.804	0.050	0.014	0.018	0.030	
															-1.5	1	1	1	1	1	0.987	0.171	0.021	0.030		
															-1.75	1	1	1	1	1	1	0.998	0.946	0.060		

FIG. A1. The results of learning a thousand of random pure states obtained without the RL agent. The target success count is set to $C_{\text{target}} = 10^4$. We express the average of total success count and infidelity on a logarithmic scale. The total time steps are represented by ratio t_H/t_{max} , where $t_{\text{max}} = 10^4$, 10^5 , and 10^6 for 1-, 2-, and 3-qubit state, respectively. The shaded cells are where the evolution strategy fails to learn quantum states within the maximum time step. The columns (a)–(c) are the results of the learning 1-, 2-, and 3-qubit states with the 16 actions, respectively. The column (d) is the result of the learning 2-qubit states with the 169 actions. The baseline values and corresponding action a_{base} are represented by the red fonts.

- \mathcal{A} is the space of action $a_t = (\sigma_t, \eta_t)$, where σ and η are hyperparameters of evolution strategy which determine *sampling range* and *learning rate*, respectively [43].
- \mathcal{T} is the space of transition probability defined by $p(s_{t+1}|s_t, a_t) : \mathcal{S} \times \mathcal{A} \times \mathcal{S} \rightarrow [0, 1]$.
- \mathcal{R} is the space of reward r_t . The reward $r_t = 0$ if the learning quantum states is finished at time step t . Otherwise, $r_t = -1$.
- Ω is the space of observation o_t . To observe the state, we use a measurement of binary outcome; *success* and *fail*. We perform the measurement until the fail outcome appears. The observation is the number of consecutive success outcomes before a fail outcome appears.
- \mathcal{O} is the space of the transition probability of observation defined by $p(o_t|s_t) : \mathcal{O} \times \mathcal{S} \rightarrow [0, 1]$.

Appendix C: Actor-Critic algorithm

Actor-Critic algorithm proceeds with iteration of generating training datasets, value evaluation, and policy

improvement [87, 88]. We generate the rollout datasets $\{(o_t, a_t, r_t, o_{t+1})\}_{t=1}^{t_H-1}$ by using a tree search guided by the policy and store them in the data buffer. We randomly sample a datasets \mathcal{B} from the data buffer [89], and, based on the sampled datasets \mathcal{B} , the critic network evaluates the observation-value function Q_{ϕ_1} . We take the empirical cumulative reward (9) as an estimator of the observation-value function:

$$\tilde{Q}(o_t) = \frac{\mathcal{R}_t}{t_{\text{max}}}, \quad (\text{A1})$$

where t_{max} is the maximum time step of ES which is set to 3×10^3 , 10^4 , and 2×10^4 for 1-, 2-, and 3-qubit, respectively. We introduce t_{max} in the denominator to normalize the empirical cumulative reward. The loss function of critic network is given by the difference between the output of critic network and the estimator of observation-value function, i.e.,

$$\text{loss}_{\text{critic}}(\phi_1) := \frac{1}{2} \left(Q_{\phi_1}(o_t) - \tilde{Q}(o_t) \right)^2 \quad (\text{A2})$$

We update the parameters of critic network ϕ_1 by using a gradient descent method. Based on the critic network, we improve the policy π_{ϕ_2} by training the actor network. The loss function of actor network is given by

$$\text{loss}_{\text{actor}}(\phi_2) := A(o_t) \log \pi_{\phi_2}(a_t|o_t), \quad (\text{A3})$$

where $A(o_t) := Q_{\phi_1}(o_t) - \tilde{Q}(o_t)$ is called advantage. The parameters of actor network ϕ_2 is updated by a gradient ascent. In the typical Advantage Actor Critic (A2C) method [90], the value function and advantage are estimated by using the time difference (TD) error. In our case, we estimate these quantities based on the empirical value function obtained by a policy-guided tree search, similar to RL using Monte-Carlo tree search [79, 91]. We use the ADAM optimizer for the gradient methods [92]. The learning rate of ADAM optimizer is set to 10^{-4} for the learning 1-qubit states, and 3×10^{-5} for the learning 2- and 3-qubit states.

Appendix D: Learning quantum states without RL agent

In Fig. A1, we investigate the performance of learning a thousand random pure states without using the RL

agent. We choose the performance given by an action a_{base} which gives the lowest total success count as the baseline. For 1-qubit, $a_{\text{base}} = (\sigma = 0.1, \eta = 0.01)$. In case of 2-qubit, $a_{\text{base}} = (\sigma = 0.1, \eta = 0.001)$ for the 16 actions, and $a_{\text{base}} = (\sigma = 10^{-1}, \eta = 10^{-2.75})$ for the 169 actions. For 3-qubit, $a_{\text{base}} = (\sigma = 0.033, \eta = 0.0001)$. The respective baseline values are represented by the red fonts in Fig. A1, and the dashed lines in Fig. 2. The shaded cells are where the evolution strategy fails to learn quantum states within the maximum time step t_{max} . These results imply that, without the RL agent, finding an action which can successfully complete the learning quantum states requires much amount of computational resources. For example, without the trained RL agent, learning a thousand 3-qubit states requires more than a million time steps for most of the actions considered.

-
- [1] A. Anshu and S. Arunachalam, A survey on the complexity of learning quantum states, *Nature Reviews Physics* **6**, 59 (2024).
- [2] V. Gebhart, R. Santagati, A. A. Gentile, E. M. Gauger, D. Craig, N. Ares, L. Bianchi, F. Marquardt, L. Pezzè, and C. Bonato, Learning quantum systems, *Nature Reviews Physics* **5**, 141 (2023).
- [3] K. Vogel and H. Risken, Determination of quasiprobability distributions in terms of probability distributions for the rotated quadrature phase, *Phys. Rev. A* **40**, 2847 (1989).
- [4] Z. Hradil, Quantum-state estimation, *Phys. Rev. A* **55**, R1561 (1997).
- [5] M. Paris and J. Rehacek, *Quantum state estimation*, Vol. 649 (Springer Science & Business Media, 2004).
- [6] M. Cramer, M. B. Plenio, S. T. Flammia, R. Somma, D. Gross, S. D. Bartlett, O. Landon-Cardinal, D. Poulin, and Y.-K. Liu, Efficient quantum state tomography, *Nature Communications* **1**, 149 (2010).
- [7] B. P. Lanyon, C. Maier, M. Holzäpfel, T. Baumgratz, C. Hempel, P. Jurcevic, I. Dhand, A. S. Buyskikh, A. J. Daley, M. Cramer, M. B. Plenio, R. Blatt, and C. F. Roos, Efficient tomography of a quantum many-body system, *Nature Physics* **13**, 1158 (2017).
- [8] C. Schwemmer, G. Tóth, A. Niggebaum, T. Moroder, D. Gross, O. Gühne, and H. Weinfurter, Experimental comparison of efficient tomography schemes for a six-qubit state, *Phys. Rev. Lett.* **113**, 040503 (2014).
- [9] S. Aaronson, Shadow tomography of quantum states, in *Proceedings of the 50th annual ACM SIGACT symposium on theory of computing* (2018) pp. 325–338.
- [10] J. M. Lukens, K. J. H. Law, A. Jindra, and P. Lougovski, A practical and efficient approach for bayesian quantum state estimation, *New Journal of Physics* **22**, 063038 (2020).
- [11] C.-Y. Park and M. J. Kastoryano, Geometry of learning neural quantum states, *Phys. Rev. Res.* **2**, 023232 (2020).
- [12] S. Ahmed, C. Sánchez Muñoz, F. Nori, and A. F. Kockum, Classification and reconstruction of optical quantum states with deep neural networks, *Phys. Rev. Res.* **3**, 033278 (2021).
- [13] S. Ahmed, C. Sánchez Muñoz, F. Nori, and A. F. Kockum, Quantum state tomography with conditional generative adversarial networks, *Phys. Rev. Lett.* **127**, 140502 (2021).
- [14] P. Cha, P. Ginsparg, F. Wu, J. Carrasquilla, P. L. McMahon, and E.-A. Kim, Attention-based quantum tomography, *Machine Learning: Science and Technology* **3**, 01LT01 (2021).
- [15] H. Lange, M. Kebrič, M. Buser, U. Schollwöck, F. Grusdt, and A. Bohrdt, Adaptive Quantum State Tomography with Active Learning, *Quantum* **7**, 1129 (2023).
- [16] A. Gaikwad, O. Bihani, Arvind, and K. Dorai, Neural-network-assisted quantum state and process tomography using limited data sets, *Phys. Rev. A* **109**, 012402 (2024).
- [17] A. M. Palmieri, G. Müller-Rigat, A. K. Srivastava, M. Lewenstein, G. Rajchel-Mieldzioć, and M. Płodzień, Enhancing quantum state tomography via resource-efficient attention-based neural networks, *Phys. Rev. Res.* **6**, 033248 (2024).
- [18] H. Ma, D. Dong, I. R. Petersen, C.-J. Huang, and G.-Y. Xiang, Neural networks for quantum state tomography with constrained measurements, *Quantum Information Processing* **23**, 317 (2024).
- [19] Q.-Q. Wang, S. Dong, X.-W. Li, X.-Y. Xu, C. Wang, S. Han, M.-H. Yung, Y.-J. Han, C.-F. Li, and G.-C. Guo, Efficient learning of mixed-state tomography for photonic quantum walk, *Science Advances* **10**, ead4871 (2024).
- [20] G. Torlai, G. Mazzola, J. Carrasquilla, M. Troyer, R. Melko, and G. Carleo, Neural-network quantum state tomography, *Nature Physics* **14**, 447 (2018).
- [21] A. Rocchetto, E. Grant, S. Strelchuk, G. Carleo, and S. Severini, Learning hard quantum distributions with variational autoencoders, *npj Quantum Information* **4**, 28 (2018).
- [22] J. Carrasquilla, G. Torlai, R. G. Melko, and L. Aolita, Reconstructing quantum states with generative models, *Nature Machine Intelligence* **1**, 155 (2019).

- [23] A. M. Palmieri, E. Kovlakov, F. Bianchi, D. Yudin, S. Straupe, J. D. Biamonte, and S. Kulik, Experimental neural network enhanced quantum tomography, *npj Quantum Information* **6**, 20 (2020).
- [24] X. Gao and L.-M. Duan, Efficient representation of quantum many-body states with deep neural networks, *Nature Communications* **8**, 662 (2017).
- [25] S. M. Lee, J. Lee, and J. Bang, Learning unknown pure quantum states, *Phys. Rev. A* **98**, 052302 (2018).
- [26] S. M. Lee, H. S. Park, J. Lee, J. Kim, and J. Bang, Quantum state learning via single-shot measurements, *Phys. Rev. Lett.* **126**, 170504 (2021).
- [27] Y. Liu, D. Wang, S. Xue, A. Huang, X. Fu, X. Qiang, P. Xu, H.-L. Huang, M. Deng, C. Guo, X. Yang, and J. Wu, Variational quantum circuits for quantum state tomography, *Phys. Rev. A* **101**, 052316 (2020).
- [28] S. Xue, Y. Liu, Y. Wang, P. Zhu, C. Guo, and J. Wu, Variational quantum process tomography of unitaries, *Phys. Rev. A* **105**, 032427 (2022).
- [29] N. Innan, O. I. Siddiqui, S. Arora, T. Ghosh, Y. P. Koçak, D. Paragas, A. A. O. Galib, M. A.-Z. Khan, and M. Ben-nai, Quantum state tomography using quantum machine learning, *Quantum Machine Intelligence* **6**, 28 (2024).
- [30] K. H. Wan, O. Dahlsten, H. Kristjánsson, R. Gardner, and M. S. Kim, Quantum generalisation of feedforward neural networks, *npj Quantum Information* **3**, 36 (2017).
- [31] K. Beer, D. Bondarenko, T. Farrelly, T. J. Osborne, R. Salzmänn, D. Scheiermann, and R. Wolf, Training deep quantum neural networks, *Nature Communications* **11**, 808 (2020).
- [32] R. Haghshenas, J. Gray, A. C. Potter, and G. K.-L. Chan, Variational power of quantum circuit tensor networks, *Phys. Rev. X* **12**, 011047 (2022).
- [33] A. Abbas, D. Sutter, C. Zoufal, A. Lucchi, A. Figalli, and S. Woerner, The power of quantum neural networks, *Nature Computational Science* **1**, 403 (2021).
- [34] E. Farhi, J. Goldstone, and S. Gutmann, A quantum approximate optimization algorithm, arXiv preprint arXiv:1411.4028 (2014).
- [35] G. Verdon, M. Broughton, J. R. McClean, K. J. Sung, R. Babbush, Z. Jiang, H. Neven, and M. Mohseni, *Learning to learn with quantum neural networks via classical neural networks* (2019), arXiv:1907.05415 [quant-ph].
- [36] M. Wilson, R. Stromswold, F. Wudarski, S. Hadfield, N. M. Tubman, and E. G. Rieffel, Optimizing quantum heuristics with meta-learning, *Quantum Machine Intelligence* **3**, 13 (2021).
- [37] S. Khairy, R. Shaydulin, L. Cincio, Y. Alexeev, and P. Balaprakash, Learning to optimize variational quantum circuits to solve combinatorial problems, in *Proceedings of the AAAI conference on artificial intelligence*, Vol. 34 (2020) pp. 2367–2375.
- [38] K. Li and J. Malik, Learning to optimize, in *International Conference on Learning Representations* (2017).
- [39] Y. Chen, M. W. Hoffman, S. G. Colmenarejo, M. Denil, T. P. Lillicrap, M. Botvinick, and N. Freitas, Learning to learn without gradient descent by gradient descent, in *International Conference on Machine Learning* (PMLR, 2017) pp. 748–756.
- [40] A. W. R. Smith, J. Gray, and M. S. Kim, Efficient quantum state sample tomography with basis-dependent neural networks, *PRX Quantum* **2**, 020348 (2021).
- [41] Y. Quek, S. Fort, and H. K. Ng, Adaptive quantum state tomography with neural networks, *npj Quantum Information* **7**, 105 (2021).
- [42] A. Kandala, A. Mezzacapo, K. Temme, M. Takita, M. Brink, J. M. Chow, and J. M. Gambetta, Hardware-efficient variational quantum eigensolver for small molecules and quantum magnets, *Nature* **549**, 242 (2017).
- [43] T. Salimans, J. Ho, X. Chen, S. Sidor, and I. Sutskever, Evolution strategies as a scalable alternative to reinforcement learning, arXiv preprint arXiv:1703.03864 (2017).
- [44] S. Narvekar, B. Peng, M. Leonetti, J. Sinapov, M. E. Taylor, and P. Stone, Curriculum learning for reinforcement learning domains: a framework and survey, *J. Mach. Learn. Res.* **21** (2020).
- [45] J. Haah, A. W. Harrow, Z. Ji, X. Wu, and N. Yu, Sample-optimal tomography of quantum states, *IEEE Transactions on Information Theory* **63**, 5628 (2017).
- [46] R. S. Sutton and A. G. Barto, *Reinforcement learning: An introduction* (MIT press, 2018).
- [47] R. Bellman, The theory of dynamic programming, *Bulletin of the American Mathematical Society* **60**, 503 (1954).
- [48] K. J. Åström, Optimal control of markov processes with incomplete state information ii: The convexity of the loss-function, *Journal of Mathematical Analysis and Applications* **26**, 403 (1969).
- [49] M. Hausknecht and P. Stone, Deep recurrent q-learning for partially observable mdps, in *2015 aaii fall symposium series* (2015).
- [50] J. Barry, D. T. Barry, and S. Aaronson, Quantum partially observable markov decision processes, *Phys. Rev. A* **90**, 032311 (2014).
- [51] V. V. Sivak, A. Eickbusch, H. Liu, B. Royer, I. Tsioutsios, and M. H. Devoret, Model-free quantum control with reinforcement learning, *Phys. Rev. X* **12**, 011059 (2022).
- [52] M. Bukov, A. G. R. Day, D. Sels, P. Weinberg, A. Polkovnikov, and P. Mehta, Reinforcement learning in different phases of quantum control, *Phys. Rev. X* **8**, 031086 (2018).
- [53] T. Fösel, P. Tighineanu, T. Weiss, and F. Marquardt, Reinforcement learning with neural networks for quantum feedback, *Phys. Rev. X* **8**, 031084 (2018).
- [54] M. Y. Niu, S. Boixo, V. N. Smelyanskiy, and H. Neven, Universal quantum control through deep reinforcement learning, *npj Quantum Information* **5**, 33 (2019).
- [55] Z. T. Wang, Y. Ashida, and M. Ueda, Deep reinforcement learning control of quantum cartpoles, *Phys. Rev. Lett.* **125**, 100401 (2020).
- [56] R. Porotti, A. Essig, B. Huard, and F. Marquardt, Deep Reinforcement Learning for Quantum State Preparation with Weak Nonlinear Measurements, *Quantum* **6**, 747 (2022).
- [57] F. Metz and M. Bukov, Self-correcting quantum many-body control using reinforcement learning with tensor networks, *Nature Machine Intelligence* **5**, 780 (2023).
- [58] W. Vent, Rechenberg, ingo, evolutionsstrategie — optimierung technischer systeme nach prinzipien der biologischen evolution. 170 s. mit 36 abb. frommann-holzboog-verlag. stuttgart 1973. broschiert, *Feddes Repertorium* **86**, 337 (1975).
- [59] N. Hansen, The cma evolution strategy: A tutorial, arXiv preprint arXiv:1604.00772 (2016).
- [60] K. Mitarai, M. Negoro, M. Kitagawa, and K. Fujii, Quantum circuit learning, *Phys. Rev. A* **98**, 032309 (2018).

- [61] M. Schuld, V. Bergholm, C. Gogolin, J. Izaac, and N. Killoran, Evaluating analytic gradients on quantum hardware, *Phys. Rev. A* **99**, 032331 (2019).
- [62] J. R. McClean, S. Boixo, V. N. Smelyanskiy, R. Babush, and H. Neven, Barren plateaus in quantum neural network training landscapes, *Nature Communications* **9**, 4812 (2018).
- [63] M. Cerezo and P. J. Coles, Higher order derivatives of quantum neural networks with barren plateaus, *Quantum Science and Technology* **6**, 035006 (2021).
- [64] A. Arrasmith, M. Cerezo, P. Czarnik, L. Cincio, and P. J. Coles, Effect of barren plateaus on gradient-free optimization, *Quantum* **5**, 558 (2021).
- [65] A. Anand, M. Degroote, and A. Aspuru-Guzik, Natural evolutionary strategies for variational quantum computation, *Machine Learning: Science and Technology* **2**, 045012 (2021).
- [66] J. Xie, C. Xu, C. Yin, Y. Dong, and Z. Zhang, Natural evolutionary gradient descent strategy for variational quantum algorithms, *Intelligent Computing* **2**, 0042 (2023).
- [67] F. Mezzadri, How to generate random matrices from the classical compact groups (2007), arXiv:math-ph/0609050 [math-ph].
- [68] A. Paszke, S. Gross, F. Massa, A. Lerer, J. Bradbury, G. Chanan, T. Killeen, Z. Lin, N. Gimelshein, L. Antiga, et al., Pytorch: An imperative style, high-performance deep learning library, *Advances in neural information processing systems* **32** (2019).
- [69] See <https://github.com/quantum-jwjae/RL2LQS>.
- [70] S. J. Pan and Q. Yang, A survey on transfer learning, *IEEE Transactions on Knowledge and Data Engineering* **22**, 1345 (2010).
- [71] R. Zen, L. My, R. Tan, F. Hébert, M. Gattobigio, C. Miniatura, D. Poletti, and S. Bressan, Transfer learning for scalability of neural-network quantum states, *Phys. Rev. E* **101**, 053301 (2020).
- [72] A. Mari, T. R. Bromley, J. Izaac, M. Schuld, and N. Killoran, Transfer learning in hybrid classical-quantum neural networks, *Quantum* **4**, 340 (2020).
- [73] E. Bagan, M. Baig, R. Muñoz Tapia, and A. Rodriguez, Collective versus local measurements in a qubit mixed-state estimation, *Phys. Rev. A* **69**, 010304 (2004).
- [74] D. H. Mahler, L. A. Rozema, A. Darabi, C. Ferrie, R. Blume-Kohout, and A. M. Steinberg, Adaptive quantum state tomography improves accuracy quadratically, *Phys. Rev. Lett.* **111**, 183601 (2013).
- [75] K. S. Kravtsov, S. S. Straupe, I. V. Radchenko, N. M. T. Houlby, F. Huszár, and S. P. Kulik, Experimental adaptive bayesian tomography, *Phys. Rev. A* **87**, 062122 (2013).
- [76] C. Ferrie, Self-guided quantum tomography, *Phys. Rev. Lett.* **113**, 190404 (2014).
- [77] J. Shen and S. Castan, An optimal linear operator for step edge detection, *CVGIP: Graphical Models and Image Processing* **54**, 112 (1992).
- [78] S. Sharma, A. S. Lakshminarayanan, and B. Ravindran, Learning to repeat: Fine grained action repetition for deep reinforcement learning, in *International Conference on Learning Representations* (2017).
- [79] D. Silver, A. Huang, C. J. Maddison, A. Guez, L. Sifre, G. van den Driessche, J. Schrittwieser, I. Antonoglou, V. Panneershelvam, M. Lanctot, S. Dieleman, D. Grewe, J. Nham, N. Kalchbrenner, I. Sutskever, T. Lillicrap, M. Leach, K. Kavukcuoglu, T. Graepel, and D. Hassabis, Mastering the game of go with deep neural networks and tree search, *Nature* **529**, 484 (2016).
- [80] R. Porotti, V. Peano, and F. Marquardt, Gradient-ascent pulse engineering with feedback, *PRX Quantum* **4**, 030305 (2023).
- [81] I. S. Maria Schuld and F. Petruccione, An introduction to quantum machine learning, *Contemporary Physics* **56**, 172 (2015), <https://doi.org/10.1080/00107514.2014.964942>.
- [82] A. Abbas, A. Ambainis, B. Augustino, A. Bärttschi, H. Buhrman, C. Coffrin, G. Cortiana, V. Dunjko, D. J. Egger, B. G. Elmegreen, N. Franco, F. Fratini, B. Fuller, J. Gacon, C. Gonciulea, S. Gribling, S. Gupta, S. Hadfield, R. Heese, G. Kircher, T. Kleinert, T. Koch, G. Korpas, S. Lenk, J. Marecek, V. Markov, G. Mazzola, S. Mensa, N. Mohseni, G. Nannicini, C. O’Meara, E. P. Tapia, S. Pokutta, M. Proissl, P. Reberntrost, E. Sahin, B. C. B. Symons, S. Tornow, V. Valls, S. Woerner, M. L. Wolf-Bauwens, J. Yard, S. Yarkoni, D. Zechiel, S. Zhuk, and C. Zoufal, Challenges and opportunities in quantum optimization, *Nature Reviews Physics* **10.1038/s42254-024-00770-9** (2024).
- [83] Y. Chen, M. W. Hoffman, S. G. Colmenarejo, M. Denil, T. P. Lillicrap, M. Botvinick, and N. de Freitas, Learning to learn without gradient descent by gradient descent, in *Proceedings of the 34th International Conference on Machine Learning*, Proceedings of Machine Learning Research, Vol. 70, edited by D. Precup and Y. W. Teh (PMLR, 2017) pp. 748–756.
- [84] V. TV, P. Malhotra, J. Narwariya, L. Vig, and G. Shroff, Meta-learning for black-box optimization, in *Joint European Conference on Machine Learning and Knowledge Discovery in Databases* (Springer, 2019) pp. 366–381.
- [85] G. Shala, A. Biedenkapp, N. Awad, S. Adriaensen, M. Lindauer, and F. Hutter, Learning step-size adaptation in cma-es, in *Parallel Problem Solving from Nature – PPSN XVI*, edited by T. Bäck, M. Preuss, A. Deutz, H. Wang, C. Doerr, M. Emmerich, and H. Trautmann (Springer International Publishing, Cham, 2020) pp. 691–706.
- [86] R. T. Lange, T. Schaul, Y. Chen, T. Zahavy, V. Dalibard, C. Lu, S. Singh, and S. Flennerhag, Discovering evolution strategies via meta-black-box optimization, in *The Eleventh International Conference on Learning Representations* (2023).
- [87] V. Konda and J. Tsitsiklis, Actor-critic algorithms, *Advances in Neural Information Processing Systems* **12** (1999).
- [88] Z. Wang, V. Bapst, N. Heess, V. Mnih, R. Munos, K. Kavukcuoglu, and N. De Freitas, Sample efficient actor-critic with experience replay, *Proceedings of the International Conference on Learning Representations (ICLR)* (2017).
- [89] V. Mnih, K. Kavukcuoglu, D. Silver, A. A. Rusu, J. Veness, M. G. Bellemare, A. Graves, M. Riedmiller, A. K. Fidjeland, G. Ostrovski, S. Petersen, C. Beattie, A. Sadik, I. Antonoglou, H. King, D. Kumaran, D. Wierstra, S. Legg, and D. Hassabis, Human-level control through deep reinforcement learning, *Nature* **518**, 529 (2015).
- [90] V. Mnih, A. P. Badia, M. Mirza, A. Graves, T. Lillicrap, T. Harley, D. Silver, and K. Kavukcuoglu, Asynchronous methods for deep reinforcement learning, in *Proceedings*

- of The 33rd International Conference on Machine Learning*, Proceedings of Machine Learning Research, Vol. 48, edited by M. F. Balcan and K. Q. Weinberger (PMLR, New York, New York, USA, 2016) pp. 1928–1937.
- [91] L. Kocsis and C. Szepesvári, Bandit based monte-carlo planning, in *Machine Learning: ECML 2006*, edited by J. Fürnkranz, T. Scheffer, and M. Spiliopoulou (Springer Berlin Heidelberg, Berlin, Heidelberg, 2006) pp. 282–293.
- [92] D. P. Kingma and J. Ba, Adam: A method for stochastic optimization, arXiv preprint arXiv:1412.6980 (2014).